Observed and modeled evolution of the tropical mean radiation budget at the top of the atmosphere since 1985

Natalia Andronova,[1] Joyce E. Penner,[1] and Takmeng Wong[2]

Received 29 November 2008; revised 6 May 2009; accepted 8 May 2009; published 23 July 2009.

[1] We have used satellite-based broadband radiation observations to construct a long-term continuous 1985–2005 record of the radiative budget components at the top of the atmosphere for the tropical region (20°S–20°N). On the basis of the constructed record we have derived the most conservative estimate of their trends. We compared the interannual variability of the net radiative fluxes at the top of the tropical atmosphere with model simulations from the Intergovernmental Panel on Climate Change fourth assessment report (AR4) archive available up to 2000 and showed that most of the models capture the 1991 Mount Pinatubo eruption signal in both its timing and amplitude; however, none of them simulate the observed trends. Further comparison showed that among the ''best skilled'' models, which are those that showed the highest value of the correlation in simulating one or all of the observed net, shortwave, and longwave radiative fluxes at the top of the atmosphere, the model with an equilibrium climate sensitivity ~3.4°C for the doubling CO_2 represents the observed amplifying total feedback effect in the tropical atmosphere better than the models with a climate sensitivity ~2.7°C or 4.3°C. This total feedback effect was calculated on the basis of an assumed simplified system of interactions between the near-surface temperature and the net radiation at the top of the atmosphere.

Citation: Andronova, N., J. E. Penner, and T. Wong (2009), Observed and modeled evolution of the tropical mean radiation budget at the top of the atmosphere since 1985, *J. Geophys. Res.*, *114*, D14106, doi:10.1029/2008JD011560.

1. Introduction

[2] The Earth's climate system is driven by the incoming solar radiation at the top of the atmosphere (TOA). About thirty percent of the incoming solar radiation is reflected back to space while the rest is absorbed and reemitted by the Earth's climate system. The TOA net radiation absorbed by the Earth's climate system is made up of two components: absorbed shortwave radiation (i.e., incoming solar radiation minus reflected solar/shortwave radiation) and outgoing longwave (thermal) radiation. The amount of solar radiation reflected back to space and the thermal energy emitted by the Earth's climate system depends on the state of the Earth surface and atmosphere at any particular moment. A transient change in the balance between the incoming and outgoing radiation is an important indicator of the changing Earth climate, and thus is widely used for verification and validation general circulation models (GCMs).

[3] Reliable satellite measurements of the broadband radiative balance components at the TOA started in the late 1970s on board several missions. Nimbus 7 provided the first long-term satellite climate record (1978–1991), but only its global outgoing longwave (LW) radiation record is reliable because its shortwave measurements did not have an onboard shortwave calibration source. The Earth Radiation Budget Experiment (ERBE) instrument on the Earth Radiation Budget Satellite (ERBS) has the longest and most complete record (1985–1999) of radiative budget variables: reflected shortwave (SW) and outgoing total radiation (LW + SW), which allows one to estimate the outgoing LW radiation. The ERBE instrument missions were followed by the Clouds and the Earth's Radiant Energy System (CERES) instruments on the Tropical Rainfall Measurement Mission (TRMM, 1998), TERRA (2000–present), and Aqua (2002–present) satellites. Both ERBE and CERES have an onboard calibration system (SW and total) to monitor the stability of the instrument and hence are the most reliable for long-term climate change study. The CERES instrument, in general, has better absolute calibration than the ERBE instrument because of better prelaunch radiometric characterization of the instrument.

[4] A few sources of uncertainties were reported for the ERBS satellite. The first was a drift of the ERBE/ERBS altitude and a small shortwave dome degradation issue [*Wong et al.*, 2006], that required the introduction of a small correction to the data and which slightly decreased the amplitude of the outgoing LW radiation. The second source was related to the necessity of turning off the ERBE instrument in 1993 for half of a year to investigate an anomalous battery condition, that introduced some discontinuity into the data. In addition, the discontinuity between the end of the ERBE/ERBS and beginning of the CERES/TERRA measurements does not allow them to be directly combined onto the same radiometric scale.

[1] Atmospheric, Oceanic and Space Sciences, University of Michigan, Ann Arbor, Michigan, USA.
[2] NASA Langley Research Center, Hampton, Virginia, USA.

0148-0227/09/2008JD011560

[5] The first goal of this paper is to revisit the satellite-based broadband radiation observations and to construct a long-term continuous radiative budget record at the TOA, which is needed for studying trends in the Earth's climate system. The second goal is to compare the observed radiative budget at the TOA with those given by the model simulations, produced by more than a dozen coupled atmosphere-ocean general circulation models (OAGCM) for the Intergovernmental Panel on Climate Change (IPCC) fourth assessment report (AR4; http://www.mad.zmaw.de/IPCC_DDC/html/ddc_gcmdata.html). We use only those OAGCM experiments where most of natural and anthropogenic influences on the global and regional radiative forcing are taken into account, and we limit our study to the 20°S–20°N region where the ERBS satellite record has the best coverage [*Wong et al.*, 2006]. The third goal of the paper is to estimate the models' ability to reproduce the observed feedback mechanism between the near-surface temperature and the net radiation at the top of the atmosphere, and thus to evaluate indirectly the model's equilibrium climate sensitivity to the doubling of carbon dioxide.

[6] In this paper we analyze the observed decadal variability of the radiative budget at the TOA and compare it with AR4 models. One of the first analyses of the ERBS and TERRA data were presented by *Wielicki et al.* [2002] and *Lin et al.* [2004]. They showed that during 1985–1999, there was a steady increase in tropical mean TOA outgoing LW radiation with large variations because of ENSO and Mount Pinatubo eruption events. They also reported a corresponding decrease in tropical mean TOA reflected (outgoing) SW radiation during the same period. A correction to the data (mostly in the outgoing LW) due to a satellite drift [*Wong et al.*, 2006] has not changed the overall tendency in the radiative fluxes. Furthermore, on the basis of the 2000–2004 CERES/TERRA data, *Wielicki et al.* [2005] showed that the global mean TOA reflected SW radiation was continuing to decrease. However, because of the existing gaps in the data an assessment of the trends in the TOA radiative balance components was limited. Section 2 presents a method for producing a consistent compilation of these observational data into a long-term continuous record and compares decadal trends in the net radiation at TOA with other satellite-based estimations.

[7] *Wielicki et al.* [2002] was the first study to compare the observed radiative budget at TOA for 1985–1999 with the budgets simulated by a few uncoupled general circulation models with prescribed sea-surface temperatures (SST). However, the models did not explicitly include the volcanic aerosol forcing from the Mount Pinatubo eruption. *Wielicki et al.* [2002] showed that the models and observations have considerable discrepancies in their representation of the radiative fluxes at the TOA, which were hypothesized as being due to changes in the tropical cloud cover. Following this suggestion, *Clement and Soden* [2005] showed that the TOA radiative budget is not sensitive to changes in tropical convection. *Allan and Slingo* [2002] used the 1985–1998 observed and simulated OLR to show that climate models fail to reproduce the observed spatial and temporal signatures of decadal OLR variations, even when all of the currently known climate forcing agents are prescribed.

[8] In this paper, we follow the strategy taken by *Wielicki et al.* [2002] by directly comparing the observed radiative budget at the TOA with that simulated by the models, however at this time we are using more comprehensive model experiments. Section 2 presents the observations. Section 3 presents model simulations from the AR4 database and their comparison with observations. Section 4 presents a discussion and our estimation of the tropical system feedbacks, and section 5 presents our conclusions.

2. Tropical Mean Observations

[9] Analysis of the Earth's energy budget based on satellite data has great importance for climate science as it serves as a direct indicator of tendencies in the Earth's climate system evolution. It is important that along with the climate change tendencies associated with growing human activities during the ERBS period, Mount Pinatubo erupted, and during both the ERBS and TERRA periods there were two major El Nino-Southern Oscillation (ENSO) events, which left a noticeable signature on the radiative fluxes at the TOA.

[10] Figures 1a and 1b show monthly means of the outgoing longwave (LW) and shortwave (SW) radiation at the TOA in the tropics (20°S–20°N) measured by the ERBE instrument on board ERBS (ERBE/ERBS WFOV Edition3_Rev1 data set) and the CERES instrument on board TERRA (CERES/Terra ERBE-like Edition2_Rev1 data set). It can be seen that there is a discontinuity between the two data sets at the end of 1999: for the LW, the difference in the magnitude is about 4 W m^{-2}, which is above the standard deviation for both data sets; for the SW, the differences are minimal, however there is a change in tendency from a slight increase between 1995 and 1999 to a decrease between 2000 and 2005.

[11] We combined the two broadband radiation records (e.g., $x(t)$ and $y(t)$) together by applying a simple instrument absolute calibration offset correction in the following manner. First, we calculated time series means for the ERBS record from 1994 to 1999 (after the Pinatubo period), $\bar{x}$, and for the TERRA record over 2000–2005, $\bar{y}$. Then we added the differences between the original series and the means, $x(t) - \bar{x}$ and $y(t) - \bar{y}$, to the means from the other time period, $z_1(t) = \bar{y} + (x(t) - \bar{x})$ and $z_2(t) = \bar{x} + (y(t) - \bar{y})$, to obtain two versions of the record, one "ERBS-based" and the other "TERRA-based." We should note that the absolute value of the TERRA-based time series is considered to be better than that of the ERBS-based time series because of more accurate prelaunch characterization of the CERES broadband instrument as mentioned in the section 1; and also that by applying this simple calibration offset correction we might ignore the possibility that the difference between the two records is a true climate signal (direct combination of the two records is shown by *Zhang et al.* [2004]). Figures 1c and 1d show the two resulting approximations to the LW and SW time series, where remaining gaps in the monthly mean data (approximately five percent of the total data pool) were filled in by using their long-term monthly means. As mentioned earlier in the paper, the CERES instrument on the TERRA satellite is better calibrated than the ERBS nonscanner instrument. Therefore, we will focus our analysis for the rest of this section on the TERRA-based time series.

[12] Figures 2a and 2b present the entire TERRA-based record, smoothed by applying a Stineman function [*Stineman*, 1980]. Using the Stineman function is similar to a 12-month

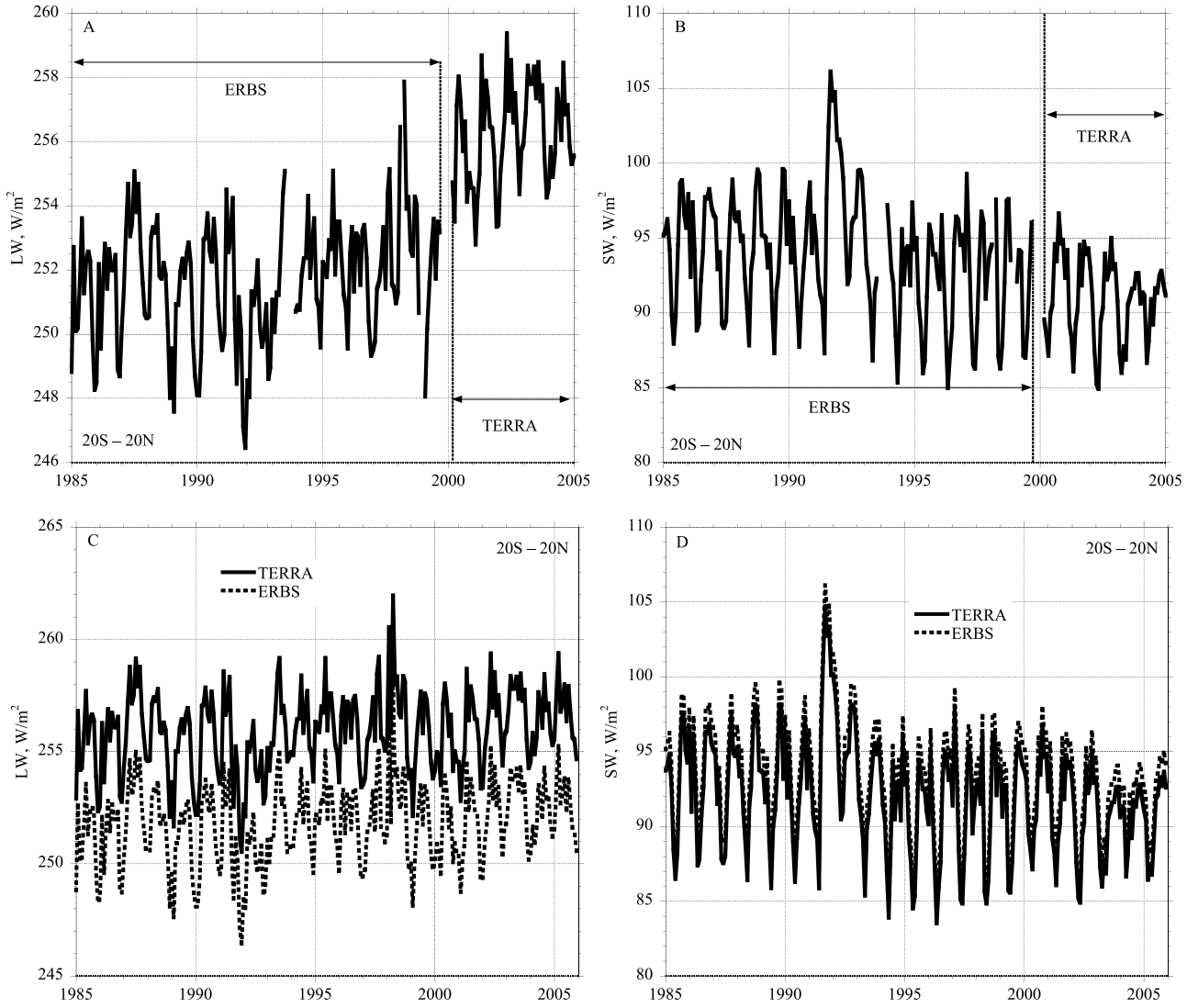

Figure 1. Satellite measurements of the (a) outgoing longwave radiation LW and (b) reflected shortwave radiation SW. (c) Outgoing longwave radiation LW and (d) the reflected shortwave radiation SW constructed using the satellite TERRA-based (solid line) and ERBS-based (dotted line) measurements at the top of the atmosphere.

smoothing of the data. In Figures 2a and 2b the gray shaded areas mark places affected by the existing gaps in the observed record. Figure 2 also shows that filling the data with the absolute maximum and absolute minimum values rather than the mean values for each month only slightly influences the trend, the significance of which we discuss below. This indicates that our procedure for merging the two records together has not distorted the overall tendency.

[13] In Figure 2a we compared the TERRA-based outgoing LW at the TOA with the NOAA High Resolution Infrared Radiation Sounder (HIRS) instrument OLR data constructed independently by *Lee et al.* [2004, 2007] using measurements from NOAA polar orbiting satellites for the period 1980–2005. These data correspond reasonably well to our TERRA-based time series, as constructed above, until 1998. After that time period the HIRS data suggest higher outgoing LW radiation. While this disagreement may indicate possible problem in our current technique for merging the TERRA and ERBS data sets, it is more likely that the cause of this disagreement is rooted in the HIRS OLR data itself. The NOAA HIRS OLR time series is derived from HIRS narrowband radiances using a multispectral regression technique [*Lee et al.*, 2007]. New regression coefficients for each satellite are derived separately using an improved radiative transfer model to capture the changes in each HIRS channel. Intersatellite calibrations were performed to remove possible bias between different satellites. However, the constant changes in the HIRS channel lineup have continued to create data quality problems for this long-term data set. *Lee et al.* [2007] noted that a shift of channel 12 of the HIRS/3 instruments, which were used on all NOAA satellites launch after October 1998, to slightly toward the center of the 6.3 um water vapor band can cause this channel to be sensitive to water vapor variation at a relatively higher altitude. This may change the HIRS's OLR sensitivity to the upper tropospheric humidity variation. In addition, the change in the channel 10 lineup from 8.2 um on the HIRS/2 instrument to 12.6 um on the HIRS/2I, and HIRS/3 instrument might have caused the

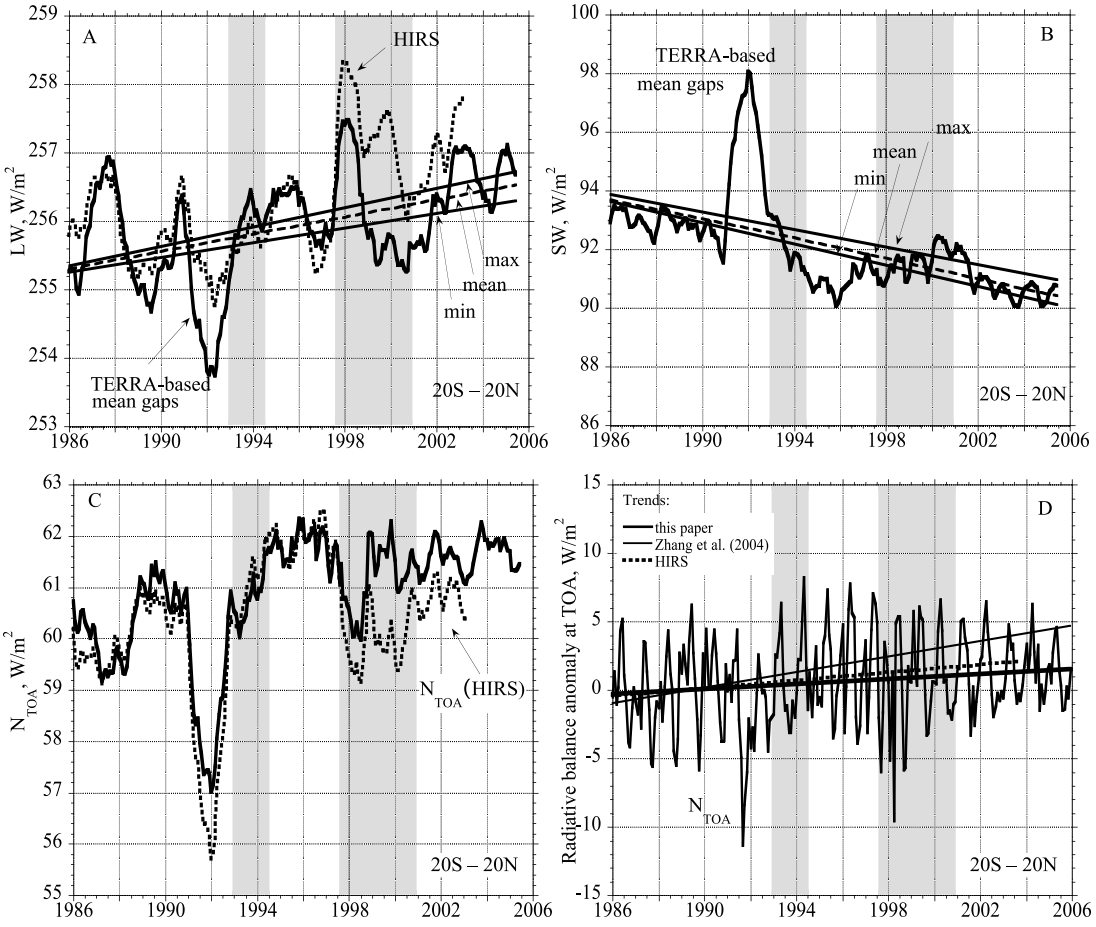

Figure 2. The 12-month smoothed TERRA-based radiative fluxes with a linear fit to the data filled with the climatological annual minimum, maximum, and mean values: (a) LW (solid curve) in comparison with High Resolution Infrared Radiation Sounder (HIRS) data (dotted curve) [*Lee et al.*, 2004, 2007] and (b) SW (solid curve). The radiative balance at TOA, N_{TOA} = SI − (LW + SW): (c) in absolute units (SI = 408.9 W m^{-2}) with a 12-month smoothing applied (the dotted line is N_{TOA} estimated using the HIRS LW) and (d) N_{TOA} 1985–1989–based anomaly as derived from the satellite observations and trends. The thick line is the trend estimated in this paper; the dotted line is the trend derived using HIRS LW; and the thin solid line is the trend derived using ISCCP-FD LW [*Zhang et al.*, 2004]. Grey shades show where the gaps in the data influence the 12-month smoothed record.

HIRS OLR algorithm to inaccurately estimate the contribution from the surface emission. These two changes may have contributed to the elevated HIRS OLR time series in the latter part of the record.

[14] As shown previously [*Wielicki et al.*, 2002; *Wong et al.*, 2000], very clear signals from the Mount Pinatubo eruption (in both the LW and SW fields) and from the 1986/1987 and 1997/1998 ENSO events (in the LW field) are apparent in the radiative energy budget data. Figures 2a and 2b show that in contrast to the LW, which has comparable sensitivities to ENSO events (of order 2 W m^{-2}) and to the stratospheric aerosol resulting from a volcanic eruption (of order 4 W m^{-2}), the reflected SW radiation is much more sensitive to the Pinatubo stratospheric aerosol (of order 6 W m^{-2}) than it is to a possible modification of the cloud cover due to ENSO events. At the time of the volcanic eruption and for at least 2 years thereafter, there is a significantly higher reflection of the incoming solar radiation to space.

[15] Computing the radiation budget at the top of the atmosphere requires an estimate of the TOA solar irradiance (SI). The average tropical mean (20°N–20°S) incoming solar radiation is 410.3 W m^{-2} with a 1-σ uncertainty of 1.3 W m^{-2}. This range of values was estimated from the following sources. The long-term mean solar constant value determined by the ERBE/ERBS solar irradiance sensor from 1984 to 2004 is 1365.4 W m^{-2} with 0.1% variability due to the 10-year sunspot cycle [*Lee and Wilson*, 2004]. This is similar (within 1 W m^{-2}) to that from ACRIM-II over the time period 1991–1999 (http://eosweb.larc.nasa.gov/PRODOCS/acrimII/table_acrimII.html). The lowest value of the solar constant was measured by TIM/SORCE which reported the value ~1360.8 W m^{-2} over period 2003–2007. This can be compared with the Nimbus 7 ERB measurements of 1372.1 W m^{-2} over period 1978–1985 [*Fröhlich*, 2003; *Kopp et al.*, 2005] (see data available at ftp://ftp.pmodwrc.ch/pub/data/irradiance/composite/). The Nimbus 7 ERB SI value is generally consider to be too high since it is an earlier

Table 1. Significance of the Radiative Flux Trend at the Top of the Tropical Atmosphere, Computed Using a Student's *t* Test

	SW	LW	N_{TOA} (This Paper)	N_{TOA} [*Zhang et al.*, 2004]
	PVT: Test for the Paired Data With Unequal Variances (Degree of Freedom = 251)			
|t| value	0.0557	0.0210	0.0793	0.0404
T probability	0.956	0.983	0.937	0.968
	UMT: Test for the Unpaired Data With Unequal Means (Degree of Freedom = 502)			
|t| value	0.0101	0.0032	0.0096	0.0126
T probability	0.992	0.999	0.992	0.990

instrument and its absolute calibration is not quite as good as the newer instruments. As we show in section 3, different GCMs use different values of SI for tuning, but they are within this range of uncertainty. For this study, we use the latest tropical mean solar irradiance value of 408.9 W m^{-2}, which is closer to the lower limit of the above range.

[16] Figure 2c presents the net radiative balance at the top of the atmosphere, N_{TOA} = SI − (LW + SW), defined as the difference in the incoming (SI) and outgoing (LW plus SW) radiation smoothed with a 12-month smoothing. Similar to the Figures 2a and 2b, the gray windows in Figure 2c correspond to years where the lack of data in the satellite record required data filling. As can be seen, N_{TOA} preserves the signature of the Mount Pinatubo eruption, which corresponds to the absolute minimum in the radiative balance time series over 1985–2005, as well as the signatures of the ENSO events during 1987–1988 and 1997–1998; both phenomena are responsible for a reduction of N_{TOA}.

[17] Figure 2d presents the N_{TOA} unsmoothed observed anomaly (relative to the average over 1985–1989), which, can be seen to have gained on the order of 2 W m^{-2} relative to 1985. The overall increase in the net incoming radiative energy in the tropics over 1985–2005 is primarily due to the decrease in the reflected shortwave radiation, which was about 3 W m^{-2} (see Figure 2b) in comparison with the smaller increase in the outgoing LW of about 1 W m^{-2} (see Figure 2a). Figure 2d also shows the trend plotted with the use of HIRS [*Lee et al.*, 2004, 2007] and the ISCCP-FD [*Zhang et al.*, 2004] outgoing LW data. The ERBS/TERRA record constructed here has the most conservative increase in N_{TOA}. While the changes in the SW flux from 1980 to 1990 may be attributed to a trend in tropospheric aerosol and related to indirect cloud effects [*Mishchenko et al.*, 2007] and the changes in general circulation [*Chen et al.*, 2002], the cause of the LW flux changes may be related to changes in both the tropical hydrological cycle [*Wild et al.*, 2008] and tropical convection [*Allan and Slingo*, 2002]. Another factor, that might be important for the tropical decadal LW variability is the low-frequency climate signal discovered by [*Zhang et al.*, 1997; *Mantua et al.*, 1997] and was derived as the leading principle component of monthly SST anomalies in the North Pacific Ocean. Thus, the decadal changes in the tropical mean radiation budget are complicated and further studies are needed to pinpoint the exact cause of this variability.

[18] To examine the significance of the trends we use the standard statistical tests: the Student's *t* tests for unpaired (i.e., independent) data with unequal means and for paired (related to each other) data with unequal variances. For these we calculated (1) the data anomalies, $x_{-m} = x - \bar{x}$, where $\bar{x}$ is the mean of x over 1985–2006, and (2) the data with the trend removed, $x_{-t} = x -$ trend. We formulate the "null" hypothesis that in the first case, their resulting means ($\overline{x_{-m}}$ and $\overline{x_{-t}}$) and in the second case, their variances ($Var(x_{-m})$ and $Var(x_{-t})$) are not significantly different. We denote the *t* test for the unpaired data with unequal means as UMT, and the *t* test for paired data with unequal variance as PVT.

[19] For both *t* tests we calculated a $|t|$ value:

$$|t| = \frac{\overline{x_{-m}} - \overline{x_{-t}}}{s_D}.$$

For the UMT we use

$$s_D = \sqrt{\frac{\sum (x_{-m} - \overline{x_{-m}})^2 + \sum (x_{-t} - \overline{x_{-t}})^2}{n_{-m} + n_{-t} - 2} \left(\frac{1}{n_{-m}} + \frac{1}{n_{-t}}\right)}$$

where n_{-m} and n_{-t} are the number points of x_{-m} and x_{-t} (in our case $n_{-m} = n_{-t} = 252$, which covers 20 years of the record starting from 1985), and where $n_{-m} + n_{-t} - 2$ is the number degrees of freedom (*df*). For PVT we use

$$s_D = \sqrt{\frac{Var(x_{-m}) + Var(x_{-t}) - 2Cov(x_{-m}, x_{-t})}{n}}$$

where $df = n - 1$ and where $Cov(x_{-m}, x_{-t})$ is the covariance of x_{-m} and x_{-t}, and $n = n_{-m} = n_{-t}$.

[20] The results of these calculations are presented in Table 1. Table 1 shows that the PVT is more conservative (i.e., less significant) than the UMT. It shows that in case of the PVT, the trends in the individual outgoing radiative fluxes at the TOA are significant at greater than the 95% confidence level for both SW and LW, but not for the N_{TOA}. We should mention that the significance of the SW trend was noted by *Hegerl et al.* [2007]. The higher trend in N_{TOA} estimated by *Zhang et al.* [2004] is statistically significant at greater than the 95% confidence level. All the UMT tests are significant at greater than the 99% confidence level. It is crucial to reconcile uncertainties in the estimates of the net radiative balance at the TOA as it is an important indicator of the changing Earth climate and is an important variable for estimating climate sensitivity [*Andronova et al.*, 2007]. Section 3 compares the observed radiative balance at the top of the atmosphere with model simulations.

3. Tropical Mean Data From Model Simulations

[21] We used AR4 data from simulations of the 20th century (20c3m) for all available general circulation models. For comparison with observations we limited all the data to 20°N–20°S. We considered the following variables: the net radiative balance at the TOA, (N_{TOA}); the TOA absorbed shortwave radiation, SW_{TOA}^{abs}(= SI − SW); and the outgoing LW at the TOA. In contrast to *Wielicki et al.* [2002], we have chosen only those IPCC AR4 model simulations that include

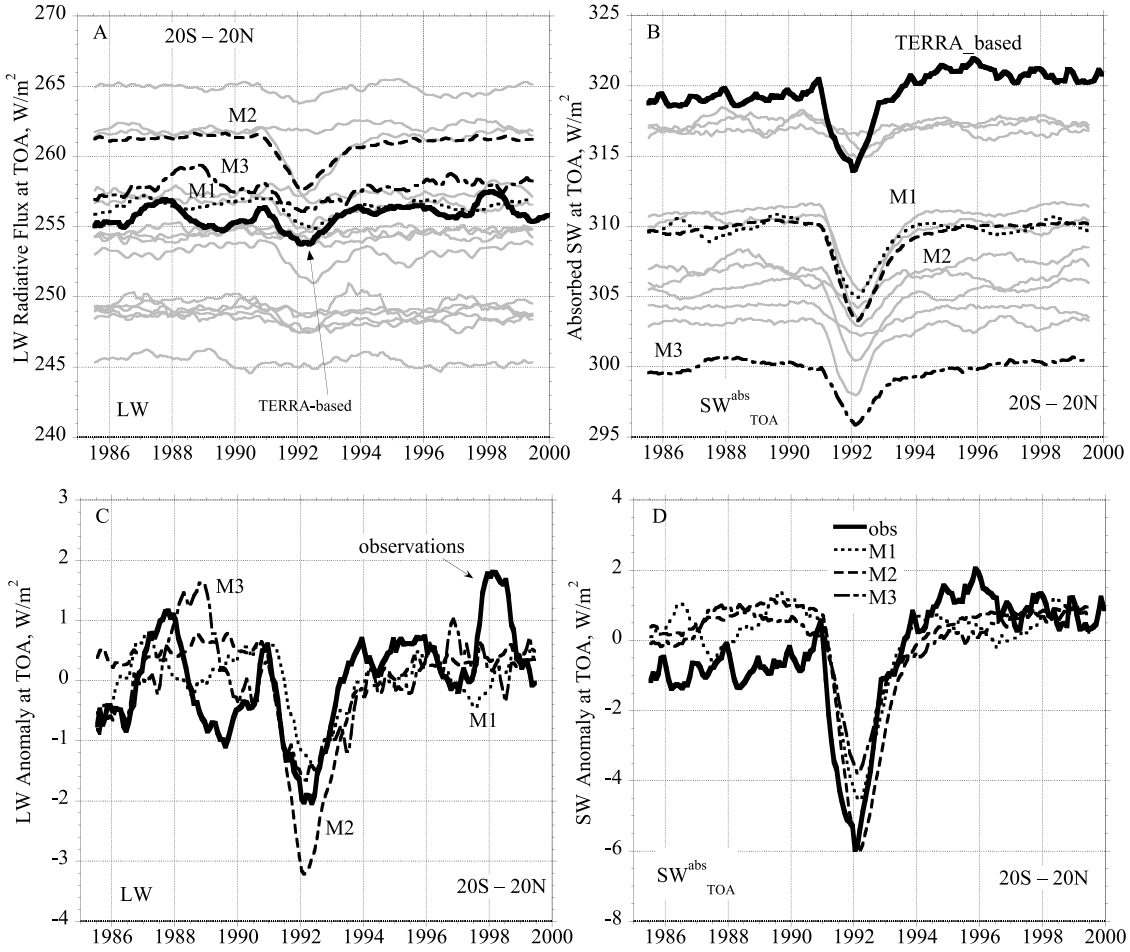

Figure 3. AR4 model simulations of LW and SW^{abs}_{TOA} at TOA (gray curves) in comparison with the TERRA-based satellite observations (thick solid curve). Dashed and dotted curves are the better model simulations (M1, M2, and M3) for the LW and SW fluxes. (a) LW absolute values, (b) SW absolute values, (c) LW anomaly over 1985–2000, and (d) absorbed SW anomaly over 1985–2000.

the effect of the Mount Pinatubo eruption, which resulted in a decrease of the outgoing LW and an increase in the outgoing SW radiation. Usually GCMs are tuned to reproduce well the present-day outgoing longwave radiation. However, each GCM group chose different observational fields to tune the model, and we demonstrate this by using the absolute values for the corresponding quantities. Also, some of the GCM groups made multiple realizations of their experiments.

[22] Figure 3a shows the 12-month smoothed absolute value of the outgoing LW at the TOA from the satellite measurements and the IPCC AR4 models (where available we used the model realization that had the highest correlation in the outgoing LW at the TOA with the observed fields). The simulated mean values vary between models from 245 W m^{-2} to 265 W m^{-2}, while the means of the two time series constructed in section 2 on the basis of the ERBS and TERRA observations (ERBS-based and TERRA-based time series) have a range from 252 W m^{-2} to 256 W m^{-2} with a standard deviation of 1.8 W m^{-2}. The TERRA-based time series is considered to be the more accurate one because of better prelaunch radiometric characterization of the CERES instrument. In Figure 3a, three model results are highlighted and marked as M1, M2, and M3. These models, in the order M2, M1, and M3, show the highest correlation (from 0.61 to 0.47) with the tropical 12-month smoothed observed TERRA-based values of the TOA LW. It can be seen that the "forced" Mount Pinatubo eruption signal is captured well by most of the models in both its timing and amplitude. However, it is still problematic for models to capture the timing and amplitude of the "unforced" ENSO events [*Wielicki et al.*, 2002]. The latter is clearly seen in Figure 3c, where (with the same highlights as in Figure 3a), the corresponding 12-month smoothed anomalies from the mean over 1985–2000 are presented. It is not expected that a GCM, coupled to an ocean, will reproduce the exact timing/amplitude of any observed ENSO events without nudging to the observed sea surface temperature, as ENSO events are regarded as an internal variability in the climate system that manifest themselves with a nonregular frequency of 3–5 years. However, the observed temporal response of the outgoing radiative fluxes at the TOA coincides with the ENSO appearance, and the magnitude of this response is comparable to the response to the Mount Pinatubo volcanic eruption, which represents an external Earth's climate system forcing.

[23] Figures 3b and 3d present SW^{abs}_{TOA} where the high-frequency seasonal variability has been removed from all

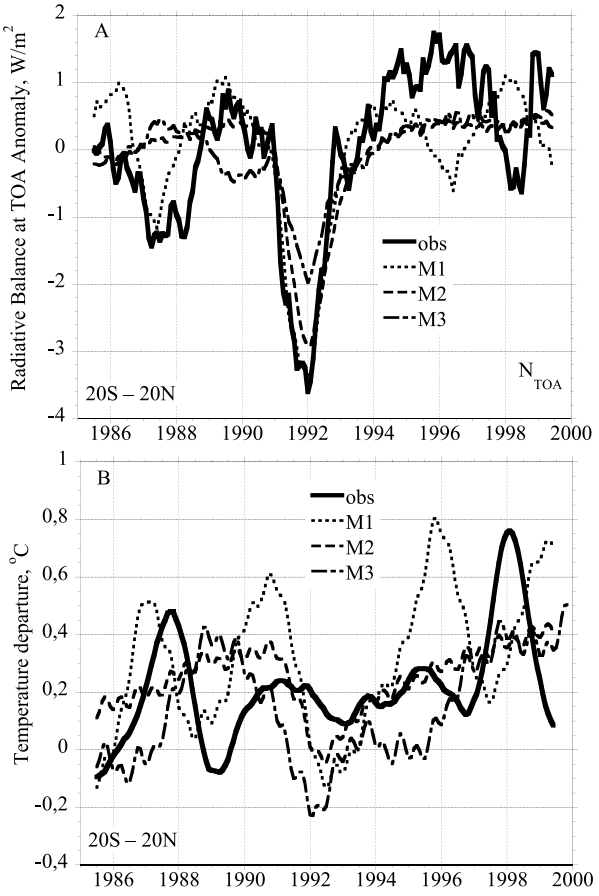

Figure 4. (a) The AR4 model-simulated N_{TOA} in comparison with the TERRA-based satellite observations (thick curves). Dashed (M2 model), dotted (M1 model), and dash-dotted (M3 model) curves are three of the better model simulations. (b) Observed (CRUT3) and simulated (ensemble mean) tropical mean near-surface temperature departures.

model simulations and TERRA-based observations by subtracting the two main modes of variability responsible for seasonal variations (the second and third eigenvectors of their covariance matrix) and then applying a 12-month smoothing. Figure 3b shows that the model's simulated absolute values of $\mathrm{SW}_{\mathrm{TOA}}^{\mathrm{abs}}$ have a much larger dispersion than the difference between the ERBS-based and TERRA-based observations derived above. The data can be divided into three parts: the pre-Pinatubo, Pinatubo and post-Pinatubo periods. The models show differences with observations in all three periods. Figure 4a presents anomalies of the TERRA-based observed and modeled (for three models M1, M2, and M3) net radiative balance at the TOA, N_{TOA}. According to the observations over 15 years, starting from 1985, the Earth's system gained approximately 1 W m^{-2} of net radiative energy, which is not seen from the models' simulations and is mainly a consequence of the lack of agreement between the simulated and observed $\mathrm{SW}_{\mathrm{TOA}}^{\mathrm{abs}}$ trends at the TOA.

[24] The overall trends simulated by the models mentioned above (M1–M3) in comparison with the observed time series constructed in this paper can be found in Table 2. It can be seen, that the trends in TOA LW, $\mathrm{SW}_{\mathrm{TOA}}^{\mathrm{abs}}$ and N_{TOA} do not agree in most cases (in general they are smaller) even with our conservative estimations.

4. Tropical Mean Climate System Feedback

[25] In section 3 we compared the tropical radiative budget at the TOA between the observations and the coupled models' simulations for the period 1985–2000. While in general the 1991 volcanic eruption of Mount Pinatubo is simulated well by the models, the long-term variability of the atmospheric-oceanic system before and after Pinatubo differs from the observed, possibly because of different feedbacks invoked by the observed and modeled systems.

[26] Below we roughly estimate the total Earth climate system feedback, L (the two-way interaction between the TOA energy budget and surface temperature), using the observed and simulated changes in N_{TOA}, ΔN_{TOA}, and the data for the observed and simulated near-surface temperature change, ΔT_s, using the cause-and-effect analysis nomenclature [*Andronova and Schlesinger*, 1991, 1992] and compare this feedback with that estimated by the models. The total feedback effect L is a useful metric for the intercomparison of models and observations, especially because $(1 - L)$ is inversely proportional to an Earth climate system response (sensitivity) to an applied disturbance [*Andronova and Schlesinger*, 1991].

[27] We use the Hadley Center CRUT3 tropical mean monthly mean near-surface temperature departures from the 1961–1990 base period [*Rayner et al.*, 2003]. To estimate the simulated near-surface temperature changes, we use the three models (M1–M3 in Figure 4a), which had the highest value of the correlation in simulating the observed radiative fluxes at the TOA. All three models reproduce the overall evolution of the tropical mean near-surface temperature departures, shown in Figure 4b for the ensemble mean. However, their absolute values for the reference period climatology differ slightly (the average temperature for M1 is 26.23°C, for M2 is 25.16°C, and for M3 is 24.89°C) in comparison with the observations (25.63°C). Thus, the M1 model represents a hotter world than that of the observations or the M2 and M3 models, and the M3 model represents a slightly colder world.

[28] Table 3 presents the simulated and TERRA-based observed averaged tropical climate for the period 1985–2000. Table 3 shows that the M1 model, while having similar cloud cover (~55%) and amount of energy absorbed by the system ($\mathrm{SW}_{\mathrm{TOA}}^{\mathrm{abs}} \sim 309$ W m^{-2}), generates a lower N_{TOA} value (~48 W m^{-2}) than the M2 model (~53 W m^{-2}) because of the difference in the outgoing longwave radiation LW and represents a warmer world (has a warmer surface) than the M2 model. The M3 model simulates the similar surface temperature as the M2 model, but it has lower cloud amount (~49%) and absorbs and emits less energy than either the M1 and M2 models. In contrast, the "real world" absorbs more

Table 2. Observed and Simulated Tropical Climate Trends Over 1985–2000[a]

	Observed	M1	M2	M3
$\mathrm{SW}_{\mathrm{TOA}}^{\mathrm{abs}} = \mathrm{SI} - \mathrm{SW}$	1.63	0.13	0.24	1.03
LW	0.76	0.12	−0.19	0.27
$N_{\mathrm{TOA}} = \mathrm{SW}_{\mathrm{TOA}}^{\mathrm{abs}} - \mathrm{LW}$	0.99	0.01	0.43	0.76

[a]Trends are W m^{-2} per decade.

Table 3. Simulated and Observed Tropical Climate Averaged Over 1985–2000 and Total Feedback Effect[a]

Name	SW^{abs}_{TOA}, W m^{-2}	LW, W m^{-2}	N_{TOA}, W m^{-2}	CL, %	T_S, °C	$L = a_{TN}a_{NT}$
obs	316 ± 4	256 ± 1	61 ± 3	61 ± 2	26 ± 0.2	L = +0.02
	absorbs the most	emits less	largest imbalance	more clouds	warm	a_{TN} = −0.0196 ± 0.04 a_{NT} = −1.02 ± 0.8
M1	309	261	48	55	26	L = +0.01
	absorbs less	emits more	smallest imbalance	less clouds	warm	a_{TN} = −0.0086 ± 0.2 a_{NT} = −1.08 ± 1.07
M2	309	256	53	55	25	L = +0.07
	absorbs less	emits less	medium imbalance	less clouds	colder	a_{TN} = +0.0251 ± 0.02 a_{NT} = +2.68 ± 1.3
M3	300	249	50	49	25	L = +0.03
	absorbs the least	emits the least	medium imbalance	the least clouds	colder	a_{TN} = +0.055 ± 1.01 a_{NT} = +0.62 ± 0.9

[a]Tropical region is 20°S–20°N.

incoming energy ($SW^{abs}_{TOA} \sim 316$ W m^{-2}) and generates more clouds (~61%, http://isccp.giss.nasa.gov/) than either of three models. If we assume that the models correctly represent the basic physical nature of the real world and generate latitudinal heat transport similar to the natural intensity, then we state the following. When comparing observations with the M2 model, to maintain a similar mean surface climate with a larger amount of energy incoming into the system, $(SW^{abs}_{TOA})_{obs} > (SW^{abs}_{TOA})_{M2}$, the Earth's climate system must spend this energy on advective processes that result in a larger cloud cover ($CL_{obs} > CL_{M2}$). Comparing the M2 and M1 models, which have similar values of the absorbed energy, SW^{abs}_{TOA}, and total cloud cover, but with the M1 surface climate warmer than the M2 climate, $(T_s)_{M1} > (T_s)_{M2}$ and with smaller outgoing *LW* in the M2 model, leads to the conclusion that the M2 model has an additional cooling factor in its system, or that the assumption about the similarity of the latitudinal heat transport between M1, M2 and real climate system does not hold. Comparing the M1 model with observations shows that consistently the smaller (larger) amount of the absorbed energy goes along with a smaller (larger) amount of clouds; a warmer (cooler) surface temperature goes along with a larger (smaller) emission of longwave radiation; and smaller (larger) amount of clouds goes along with a warmer (cooler) surface temperature. This description can also be applied to the characteristics of the M3 model.

[29] The last column of Table 3 shows our estimates for the total tropical feedback effect, L, and a comparison of the observations with the M1–M3 models. For this we collapse the Earth's climate system into a simplified two-way interaction (Figure 5) between changes in the surface climate, ΔT_s, the changes in the net radiation at the top of the atmosphere ΔN_{TOA}. We represent the system this way because (as we are showing it in Figure 5) this allows us to estimate the corresponding pathways (partial sensitivities or influences) directly from the observations. Using the nomenclature of the cause-and-effect feedback analysis [*Andronova and Schlesinger*, 1991, 1992], we denote the partial influence of ΔN_{TOA}, on ΔT_s as a_{TN} and its partial feedback (influence of ΔT_s on ΔN_{TOA}) as a_{NT}. Then the magnitude of the total feedback effect is calculated as $L = a_{NT}a_{TN}$.

[30] We should mention, that the measurements of the radiative fluxes at the TOA and the surface temperature reflect all possible competing/amplifying/controlling processes in the tropical climate system (including the latitudinal heat transport). Thus, the estimated relationships (all the "a_{ik}" coefficients) contain the effects of all the factors at work in the system. As such, the analysis is appropriate over any timescale, not just for interannual variability. *Forster and Gregory* [2006] also used the observed radiative budget derived from ERBS to estimate radiative forcing and long-

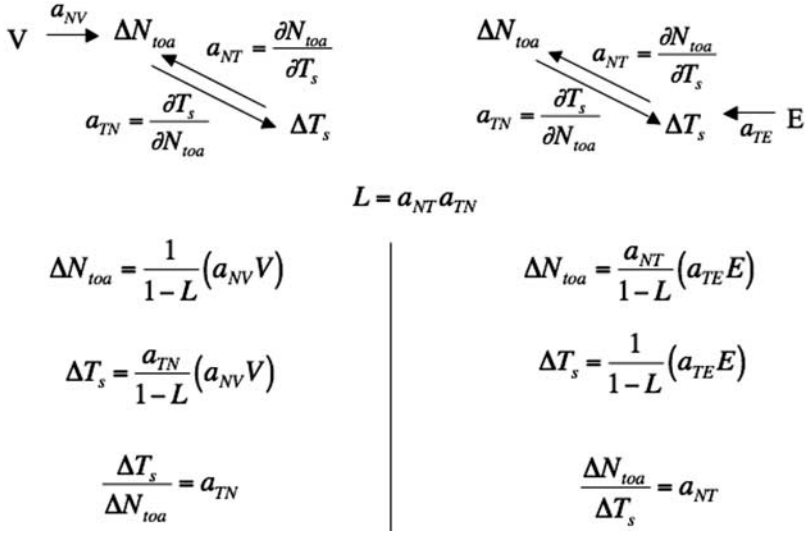

Figure 5. A simplified representation of the Earth's climate system interactions between the surface climate T_s and the net radiation at the top of the atmosphere, N_{TOA}, for two disturbances: (1) a volcanic eruption V via changes in N_{TOA} and (2) an ENSO event E via a disturbances in T_s, where L is a total feedback effect and a_{NT} and a_{TN} are partial influences of the system variables on each other.

wave feedback, but they based their analysis on a shorter observed record 1985–1996.

[31] To estimate a_{TN} we use a disturbance, V (volcano-like), via the system's node ΔN_{TOA} with an unknown transfer coefficient a_{NV}; and to estimate a_{NT} we use a disturbance E (ENSO-like) via the system's node ΔT_s with an unknown transfer coefficient a_{TE}. We assume that both "a_{NV} V" and "a_{TE}E" represent the forcing to the system of two variables during their separate respective time periods. Figure 5 outlines the relevant equations used to estimate a_{NT}, a_{TN} and the total feedback effect L.

[32] The coefficients a_{NT} and a_{TN} were estimated for two different periods: when the system was exposed to the Mount Pinatubo eruption and when a change in the surface temperature was caused by sporadic ENSO events. We do this by (1) regressing the observed and simulated changes in T_s and N_{TOA} onto each other separately for the first and second time periods to find the partial influence of the variables on each other, a_{NT} and a_{TN} and (2) finding the product of two resulting slopes, $a_{NT}a_{TN}$, which is a rough estimate of the total feedback effect, L, produced by interactions in the Earth's climate system and recorded in the cotemporal changes in T_s and N_{TOA}. We have assumed that: during the "Pinatubo" period (~1991–1993) the disturbance to the Earth's climate system was dominated by a modification of the net radiative balance at the TOA due to the volcanic aerosol (V case); and during the remaining periods (1985–1991 and 1994–2000) the disturbances to the Earth's climate system came only via a modification of the sea surface temperature (E case). We have excluded 1982/1983 years from the analysis because a strong ENSO and the Mount El Chichon eruption coincided. For the E case we considered two other cases: (E.1) the entire period before and after the Pinatubo event, and (E.2) just the ENSO years. For the time periods associated with ENSO in the models, we constructed an individual "ENSO index" based on a 3-month smoothing of the sea surface temperature for the El Nino 3.4 region (5°S–5°N, 120°–170°W), and we have chosen those time periods with a positive index (we have relaxed the definition of the index to consider just positive values, instead of the values greater than some specific value). We constructed the index for all available members of the model ensembles as well as for the ensemble mean.

[33] To estimate the partial sensitivities (a_{TN} and a_{NT}) and the total feedback effect, L, we used the 12-month smoothed data, which corresponds to the annual-mean behavior of the climate system, and thus our feedback estimation is valid on the annual timescale. For the models, we performed the analysis for both the average of the ensemble members and for each ensemble member separately followed by averaging the individual values of a_{TN} and a_{NT}. The values of the coefficients and the total feedback effect in the later case were similar to those of the former case. The values of a_{TN}, a_{NT} and L for the E.1 case when we took into account the entire period before and after the Pinatubo event for the estimation of a_{NT} were similar to the case E.2 (only ENSO years).

[34] Figure 6 shows the regression lines used for estimation of the a_{TN} and a_{NT} values in the last column of Table 3, from which it follows that the models and the observations agree on the sign of the total feedback effect L. As L is positive, the annual scale total feedback in the tropical climate system will amplify any initial disturbance introduced into the TOA energy budget (e.g., via an increased SW reflection due to the addition of stratospheric aerosol) or into the surface temperature (e.g., via a cooling/warming due to anthropogenic aerosol or ENSO). All three models in Table 3 give an approximate value of the total feedback that is correct. However, the M2 and M3 models give the "right" sign of the total feedback for the "wrong" reason: the signs of both partial sensitivities are positive in contrast to the sign for the observations. Tracking back the reasons for these discrepancies we concluded that in the M2 and M3 models the sign of a_{NT} is defined by the inability of these models to catch an ENSO-like variability in the temperature record (see Figure 4b), and the a_{TN} sign is defined by a slightly different combination of the time delay between the forcing and modeled response and the magnitude of the forcing and response during the Pinatubo period compared to the observations. The M1 model is in better agreement with the observations; however, its a_{TN} value is too small.

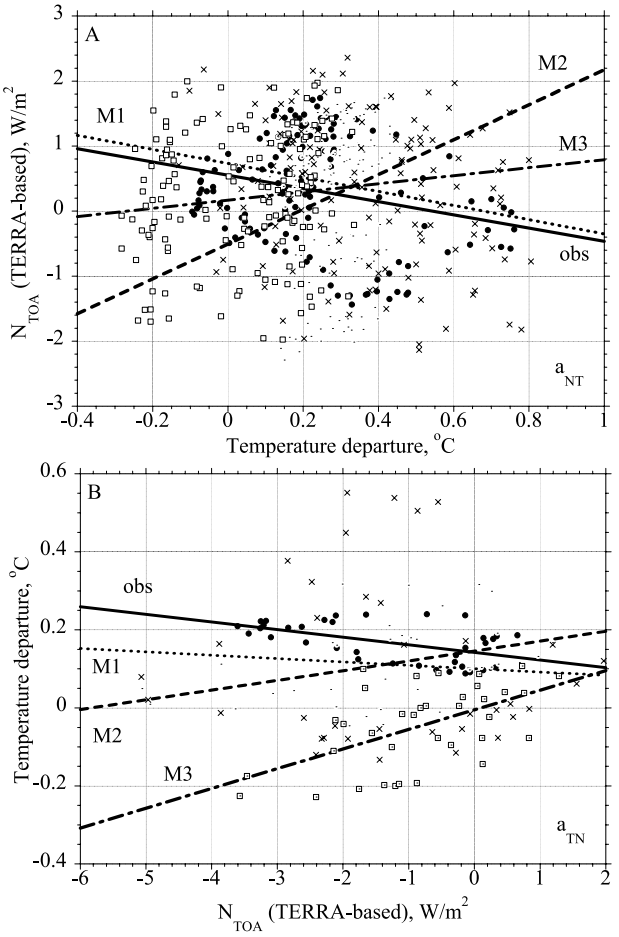

Figure 6. Scatterplot and regression lines used to estimate (a) the partial sensitivity a_{NT} using the 12-month smoothed data from the pre- and post-Pinatubo periods for the observations and the M1, M2, and M3 models and (b) the partial sensitivity a_{TN} using data from 1991 to 1993 (Pinatubo period) for the observations and the M1, M2, and M3 models.

[35] We should mention that timescales are essential to our analysis and the estimated coefficients are sensitive to

the time delay in the data: a delay between a forcing and the response that is inconsistent with the observations will be reflected in the estimated coefficients. This fact serves as a basis for the comparison of observations with models and models with each other: the larger the delay is the smaller the correlation between a forcing and a response. We estimated the time delay between the changes in the TOA radiative fluxes and the surface temperature as being 12 months, which is similar to estimates given by *Harries and Futyan* [2006].

5. Conclusions

[36] In this paper we have revisited the satellite-based broadband radiation observations and have developed long-term radiative budgets at the TOA (20 years) for the tropical region (20°S–20°N). We have also compared the radiative budget at the TOA with the AR4 historical model simulations available for 15 years during the satellite era, and derived another metric (the tropical mean total feedback effect) for model-to-model and model-to-observations intercomparisons. We have not tested the robustness of the results to the definition of the tropical regions but relied on the domain defined for the radiative fluxes in the used data sets; this should be done in the future.

[37] We used the observations to show that the tropical system became both less reflective and more absorbing at the TOA. Combined with a reduction in total cloudiness [*Norris*, 2007], this would mean that the tropical atmosphere had recently become more transparent to incoming solar radiation, which would allow more shortwave energy to reach the Earth's surface. Both of these findings are consistent with the observed near-surface temperature increase in recent years. The comparison of the TOA observations with model simulations showed that none of the models simulates the overall "net radiative heating" signature of the Earth's radiative budget over the time period from 1985 to 2000. However, the majority of the models capture the Mount Pinatubo eruption signal reasonably well in both its timing and amplitude.

[38] We have analyzed trends in the radiative fluxes at the top of the tropical atmosphere on the basis of the 20-year continuous record constructed in this paper. The trend for variations has been constructed under the assumption that the mean over the last 5 years of ERBS and that from the first 5 years of the CERES data is the same. This assumption is needed to connect these two satellite records together. This method of combining two disjointed data sets together over the 1985–2005 period is more conservative than that used by *Zhang et al.* [2004] and it reduces the overall trend in the net radiative flux at TOA from 2.8 ± 4.1 W m^{-2} per decade to 0.9 ± 3.2 W m^{-2} per decade. However, at this moment there is not enough independent information for constraining the uncertainties in estimates of this trend.

[39] Using a simplified representation of the climate system we have formulated a new metric for observation-to-model and model-to-model comparisons, the "total feedback effect". We estimated the observed total feedback effect and compared it with the three models that demonstrated the best skills in reproducing the tropical radiative fluxes at the TOA. We showed that the new metric is sensitive to the presence of a time delay in the data between a forcing and the system's response and, therefore, useful for matching observations with models or/and models with models. On the basis of the new metric we further recognized that the M1 model represents the recent observations of the tropical atmosphere better than any other model.

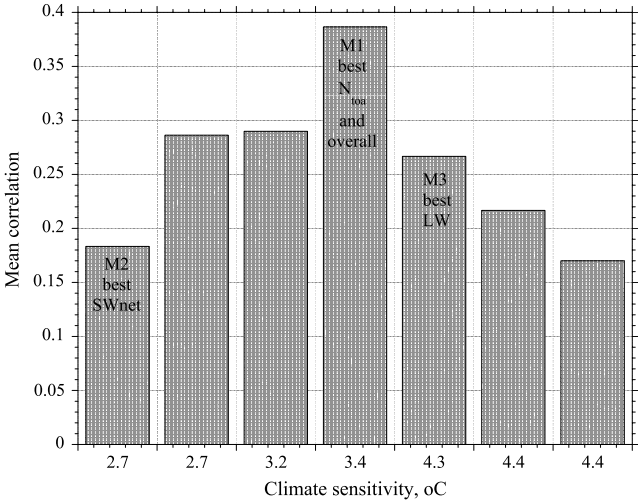

Figure 7. AR4 model's equilibrium climate sensitivity in °C versus the mean correlation of the simulated and observed tropical radiative fluxes at TOA (for any model, only one best model version is used).

[40] It is worthwhile to mention that the M1 model has an equilibrium climate sensitivity of 3.4°C defined from the doubling carbon dioxide experiments with a version of the model coupled to a slab ocean. Figure 7 shows a range of the climate sensitivity values reproduced by other AR4 models in correspondence with their mean correlation with the observed radiative fluxes at TOA. On the basis of the considered models it can be shown that better agreement of the TOA SW fluxes produces an increased climate sensitivity value, while better agreement of the TOA LW fluxes produces a decreased climate sensitivity value. According to Figure 7 the M1 model with the sensitivity 3.4°C is the best in simulating the tropical climate, the TOA tropical radiative fluxes and the tropical temperature-radiative flux interrelationship. However, the value of climate sensitivity is not, in itself, a sufficient condition for accurately reproducing regional climate conditions.

[41] **Acknowledgments.** The authors would like to thank Hai-Tien Lee (Cooperative Institute for Climate Studies, NOAA) and Yuan-Chong Zhang (Columbia University at NASA GISS) for sharing their satellite-based radiation data and William Collins (Department of Earth and Planetary Science, University of California, and Lawrence Berkeley National Laboratory) for very helpful comments and data from the AR4 database. We also express our gratitude to the anonymous reviewers for their very constructive and helpful comments. The ERBE and the CERES data are obtained from the Atmospheric Sciences Data Center at the NASA Langley Research Center in Hampton, Virginia. This work was supported by the Director, Office of Science, of the U.S. Department of Energy under contract DE-AC02-05CH11231. T. Wong is supported by the NASA Science Mission Directorate through the CERES Project at the NASA Langley Research Center.

References

Allan, R. P., and A. Slingo (2002), Can current climate model forcings explain the spatial and temporal signatures of decadal OLR variations?, *Geophys. Res. Lett.*, *29*(7), 1141, doi:10.1029/2001GL014620.

Andronova, N., and M. Schlesinger (1991), The application of cause-and-effect analysis to mathematical models of geophysical phenomena: 1. Formulation and sensitivity analysis, *J. Geophys. Res.*, *96*, 941–946, doi:10.1029/90JD02278.

Andronova, N. G., and M. E. Schlesinger (1992), The application of cause-and-effect analysis to mathematical models of geophysical phenomena: 2. Stability analysis, *J. Geophys. Res.*, *97*, 5911–5919, doi:10.1029/92JD00238.

Andronova, N., M. E. Schlesinger, S. Dessai, M. Hulme, and B. Li (2007), The concept of climate sensitivity: History and development, in *Human-Induced Climate Change: An Inter-disciplinary Assessment*, edited by M. E. Schlesinger et al., pp. 5–17, Cambridge Univ. Press, Cambridge, U. K.

Chen, J., B. E. Carlson, and A. D. Del Genio (2002), Evidence for strengthening of the tropical general circulation in the 1990s, *Science*, *295*, 838–841, doi:10.1126/science.1065835.

Clement, A. C., and B. Soden (2005), The sensitivity of the tropical-mean radiation budget, *J. Clim.*, *18*, 3189–3203, doi:10.1175/JCLI3456.1.

Forster, P. M. d. F., and J. M. Gregory (2006), The climate sensitivity and its components diagnosed from Earth radiation budget data, *J. Clim.*, *19*, 39–52, doi:10.1175/JCLI3611.1.

Fröhlich, C. (2003), Long-term behaviour of space radiometers, *Metrologia*, *40*, S60–S65, doi:10.1088/0026-1394/40/1/314.

Harries, J. E., and J. M. Futyan (2006), On the stability of the Earth's radiative energy balance: Response to the Mt. Pinatubo eruption, *Geophys. Res. Lett.*, *33*, L23814, doi:10.1029/2006GL027457.

Hegerl, G. C., F. W. Zwiers, P. Braconnot, N. P. Gillett, Y. Luo, J. A. Marengo Orsini, N. Nicholls, J. E. Penner, and P. A. Stott (2007), Understanding and attributing climate change, in *Climate Change 2007: The Physical Science Basis. Contribution of Working Group I to the Fourth Assessment Report of the Intergovernmental Panel on Climate Change*, edited by S. Solomon et al., pp. 663–748, Cambridge Univ. Press, Cambridge, U. K.

Kopp, G., G. Lawrence, and G. Rottman (2005), The Total Irradiance Monitor (TIM): Science results, *Sol. Phys.*, *230*, 129–140.

Lee, H.-T., A. Heidinger, A. Gruber, and R. G. Ellingson (2004), The HIRS outgoing longwave radiation product from hybrid polar and geosynchronous satellite observations, *Adv. Space Res.*, *33*, 1120–1124, doi:10.1016/S0273-1177(03)00750-6.

Lee, H. T., A. Gruber, R. G. Ellingson, and I. Laszlo (2007), Development of the HIRS outgoing longwave radiation climate dataset, *J. Atmos. Oceanic Technol.*, *24*, 2029–2047, doi:10.1175/2007JTECHA989.1.

Lee, R. B., III, and R. S. Wilson (2004), Validation of spacecraft active cavity radiometer total solar irradiance (TSI) long-term measurement trends using proxy TSI least squares analyses, *Proc. SPIE Int. Soc. Opt. Eng.*, *5570*, 352–362, doi:10.1117/12.565647.

Lin, B., T. Wong, B. A. Wielicki, and Y. Hu (2004), Examination of the decadal tropical mean ERBS nonscanner radiation data for the Iris hypothesis, *J. Clim.*, *17*, 1239–1246, doi:10.1175/1520-0442(2004)017<1239:EOTDTM>2.0.CO;2.

Mantua, N. J., S. R. Hare, Y. Zhang, J. M. Wallace, and R. C. Francis (1997), A Pacific interdecadal climate oscillation with impacts on salmon production, *Bull. Am. Meteorol. Soc.*, *78*, 1069–1079, doi:10.1175/1520-0477(1997)078<1069:APICOW>2.0.CO;2.

Mishchenko, M. I., I. V. Geogdzhayev, W. B. Rossow, B. Cairns, B. E. Carlson, A. A. Lacis, L. Liu, and L. D. Travis (2007), Long-term satellite record reveals likely recent aerosol trend, *Science*, *315*, 1543, doi:10.1126/science.1136709.

Norris, J. R. (2007), Observed interdecadal changes in cloudiness: Real or spurious?, in *Climate Variability and Extremes During the Past 100 Years*, edited by S. Broennimann et al., pp. 169–178, Springer, New York.

Rayner, N. A., D. E. Parker, E. B. Horton, C. K. Folland, L. V. Alexander, D. P. Rowell, E. C. Kent, and A. Kaplan (2003), Globally complete analyses of sea surface temperature, sea ice and night marine air temperature, 1871–2000, *J. Geophys. Res.*, *108*(D14), 4407, doi:10.1029/2002JD002670.

Stineman, R. W. (1980), A consistently well-behaved method of interpolation, *Creative Comput.*, *6*, 54–57.

Wielicki, B. A., et al. (2002), Evidence for large decadal variability in the tropical mean radiative energy budget, *Science*, *295*, 841–844, doi:10.1126/science.1065837.

Wielicki, B. A., T. Wong, N. Loeb, P. Minnis, K. Priestley, and R. Kandel (2005), Changes in Earth's albedo measured by satellite, *Science*, *308*, 825, doi:10.1126/science.1106484.

Wild, M., J. Grieser, and C. Schär (2008), Combined surface solar brightening and increasing greenhouse effect support recent intensification of the global land-based hydrological cycle, *Geophys. Res. Lett.*, *35*, L17706, doi:10.1029/2008GL034842.

Wong, T., D. F. Young, M. Haeffelin, and S. Weckmann (2000), Validation of the CERES/TRMM ERBE-like monthly mean clear-sky longwave dataset and the effects of the 1998 ENSO event, *J. Clim.*, *13*, 4256–4267, doi:10.1175/1520-0442(2000)013<4256:VOTCTE>2.0.CO;2.

Wong, T., B. A. Wielicki, R. B. Lee III, G. L. Smith, K. A. Bush, and J. K. Willis (2006), Re-examination of the observed decadal variability of Earth radiation budget using altitude-corrected ERBE/ERBS nonscanner WFOV data, *J. Clim.*, *19*, 4028–4040, doi:10.1175/JCLI3838.1.

Zhang, Y., J. M. Wallace, and D. S. Battisti (1997), ENSO-like interdecadal variability: 1900–93, *J. Clim.*, *10*, 1004–1020, doi:10.1175/1520-0442(1997)010<1004:ELIV>2.0.CO;2.

Zhang, Y., W. B. Rossow, A. A. Lacis, V. Oinas, and M. I. Mishchenko (2004), Calculation of radiative fluxes from the surface to top of atmosphere based on ISCCP and other global data sets: Refinements of the radiative transfer model and the input data, *J. Geophys. Res.*, *109*, D19105, doi:10.1029/2003JD004457.

N. Andronova and J. E. Penner, Atmospheric, Oceanic and Space Sciences, University of Michigan, Ann Arbor, MI 48109-2143, USA. (natand@umich. edu)

T. Wong, NASA Langley Research Center, Mail Code 420, Hampton, VA 23681-0001, USA.